Article

Not peer-reviewed version

Wound Healing Efficacy of Cellulose Hydrogel on ICR Mice: A Morphoanatomical, Histological and Genomic Study

Abigail Castro *, Alvin Domingo, Jayson Cariaga, Francis Gamboa, Aira Cassandra Castro, Aira Nadine Pascua, Jimmbeth Zenila Fabia, Peter James Gann, Bjorn Santos, Shirley Agrupis

Posted Date: 24 September 2024

doi: 10.20944/preprints202409.1941.v1

Keywords: wound healing; cellulose hydrogel; probiotics; histological assessment

Article

Wound Healing Efficacy of Cellulose Hydrogel on ICR Mice: A Morphoanatomical, Histological and Genomic Study

Abigail S. Castro [1,*], Alvin G. Domingo [1,2], Jayon F. Cariaga [1,2], Francis A. Gamboa [2], Aira Cassandra S. Castro [3], Aira Nadine Q. Pascua [1], Jimmbeth Zenila P. Fabia [4], Peter James Icalia Gann [1,4], Bjorn S. Santos [2] and Shirley C. Agrupis [1,4]

[1] Department of Biological Sciences, College of Arts and Sciences, Mariano Marcos State University, City of Batac, Ilocos Norte, Philippines
[2] National Bioenergy Research and Innovation Center, Mariano Marcos State University, City of Batac, Ilocos Norte, Philippines
[3] College of Medicine, Mariano Marcos State University, City of Batac, Ilocos Norte, Philippines
[4] Genomics and Genetic Engineering Laboratory, College of Medicine, Mariano Marcos State University, City of Batac, Ilocos Norte, Philippines
* Correspondence: castroxabigail@gmail.com

Abstract Chronic wounds remain a major challenge in healthcare, with conventional dressings often leading to infections and lacking advanced healing capabilities. This study evaluated the wound healing potential of NIMO-CH, a cellulose hydrogel derived from nipa fronds and enriched with indigenous microorganisms, particularly *Lacticaseibacillus paracasei* BCRC-16100. Using ICR mice with excisional wounds, three treatments were compared: no treatment, NIMO-CH, and DuoDERM. Results showed that NIMO-CH and DuoDERM both achieved 100% wound closure, with NIMO-CH-treated wounds showing complete healing with hair growth by day 18-20, while untreated wounds healed by day 20. Minimal scarring was observed in both NIMO-CH and DuoDERM groups. Histological analysis confirmed similar healing processes, including granulation tissue formation and moderate inflammatory responses, with no significant differences in collagen fiber orientation. Furthermore, genome sequencing revealed that *Lacticaseibacillus paracasei* BCRC-16100 contained genes sodA and gsiC, responsible for coding enzymes necessary for the wound healing process. These results suggest that NIMO-CH could be an effective alternative for wound care applications.

Keywords: wound healing; cellulose hydrogel; probiotics; histological assessment

1. Background

Chronic wounds, wounds that can be extremely hard-to-heal, remain one of the major challenges in public health, causing severe pain and difficulties. It continues to be a silent epidemic, with the occurrence of chronic wounds increasing significantly over the past few years (Järbrink et al., 2016). Worldwide, the prevalence of chronic wounds is estimated to be between 1.51 and 2.21 cases per 1000 individuals, and these numbers are projected to increase with aging populations (Martinengo et al., 2019). In the United States, approximately 2% of the entire population is affected by chronic wounds, and their adverse impact is felt on a global scale (Järbrink et al., 2019).

Meanwhile, the significant mortality rate associated with non-healing wounds in the Philippines might be attributed to the inability of many patients to afford costly medications. Furthermore, the current wound dressings available in the market today fail to address the multifaceted factors that contribute to the healing of chronic wounds. If non-healing wounds are left untreated and not managed properly, they can lead to serious medical issues, including infection, sepsis, limb amputation, and in severe cases, even death. Hence, there is a pressing need for a more specialized and innovative approach in the development of wound care products.

 doi:10.20944/preprints202409.1941.v

Currently, new approaches for treating wounds continues to be a highly researched area (Yaseen et al., 2020). Among these new approaches are the use of cellulose-based hydrogels, a linear polysaccharide that forms the main component of the cell walls of plants, through physical cross-linking, wherein a polymer network can be linked by multiple hydroxyl groups through hydrogen bonding. Cellulose-based hydrogels has gained increasing attention due to their unique properties and potential 3 applications, including its 3D structure, high water content, biocompatibility with low risk of inducing acute or chronic inflammation, low toxicity and their ability to deliver drugs and growth factors which addresses the shortcomings of the conventional dressings (Jose et al., 2020). With this, cellulose-based hydrogels hold great promise as versatile and effective materials for wound healing and are likely to play an increasingly vital role in modern medicine.

Furthermore, the growing focus on medicinal products with natural ingredients may finally give the country a cost-effective, safe and non-invasive prevention and cure against these wounds, providing a sustainable and locally sourced solution to address the limited availability of wound dressings in the Philippines. In a recent study conducted by Domingo et al., (2022), a cellulose hydrogel made from Nipa frond was developed and synthesized. To date, there had been no previous investigations into the nipa hydrogel's use in the medical field. Thus, to comprehensively understand the potential applications of probiotics integrated into the Nipa hydrogel in the medical field and to lay the groundwork for future research, a thorough investigation of its wound healing potency was essential.

This study aimed to assess the wound healing activity in the wounds of ICR mice treated with probiotic-based cellulose hydrogel derived from nipa in terms of wound contraction, morpho-anatomical assessment and effectiveness through qualitative histological assessment.

2. Methods

2.1. Genome Sequencing and Promoter Analysis of Lacticaseibacillus paracasei BCRC-16100

Capillary Sequencing. Genomic DNA (gDNA) from BCRC-1600 was isolated using the Quick-DNA Fungal/Bacterial Miniprep Kit (Zymo Research, USA) following the manufacturer's instructions. PCR amplicons were purified with AMPure XP beads (Cat. No. 163881). One microliter of the purified amplicons was analyzed on a 1% agarose gel, run at 120 V for 45 minutes, alongside the Invitrogen 1kb Plus DNA Ladder. Capillary sequencing utilized fluorescently labeled chain-terminating ddNTPs. The reaction mixture included the amplicons, corresponding primers, and the ABI BigDye® Terminator v3.1 Cycle Sequencing Kit (Cat. No. 4337455). The thermal cycler conditions were pre-hold at 4°C, 96°C for 1 minute, followed by 25 cycles of 96°C for 10 seconds, 50°C for 5 seconds, 62°C for 4 minutes, and a final hold at 4°C. Ethanol precipitation was used to eliminate unincorporated ddNTPs, excess primers, and primer dimers. Capillary electrophoresis was performed on the ABI 3730xl DNA Analyzer with a 50 cm 96-capillary array, POP7 Polymer (Cat. No. 4393714), and 3730xl Data Collection Software v3.1. Base calling was done using Sequencing Analysis Software v5.4.

Whole Genome Sequencing. Library preparation was carried out utilizing the TruSeq DNA Nano Kit (Illumina, USA), followed by sequencing on an Illumina MiSeq instrument in a paired end read format of 2 x 150 bp for 300 cycles at the Philippine Genome Center, Quezon City, Philippines.

Prediction of Promoter Elements. Bioinformatics tools, including BPROM and BLAST, were employed to predict promoter elements involved in the gene expression related to the wound-healing activity of BCRC-16100. The upstream regions of these genes were extracted from their whole genome sequences (WGS) and analyzed using the BPROM platform. The analysis identified potential –10 and –35 promoter boxes, their positions within the submitted sequences, as well as possible associated transcription factors.

 doi:10.20944/preprints202409.1941.v

2.2. Production of NIMO-CH

Production of Cellulose Hydrogel from Nipa Frond. The isolation and purification of α-cellulose from nipa fronds followed the methodology outlined by Cariaga et al. (2019), whereas the hydrogel synthesis was carried out according to the procedures established by Domingo et al. (2022).

Derivatization of Carboxymethyl (CMC) from Cellulose. The synthesis of Carboxymethylcellulose (CMC) was performed following the protocol outlined by Asl et al. (2017). Nine grams of α-cellulose powder, derived from nipa fronds, was combined with 30 ml of 40% NaOH and 270 ml of isopropanol in a beaker and stirred for 30 minutes at room temperature. Subsequently, 10.8 g of sodium monochloroacetate was added, and the mixture was stirred using a magnetic hotplate stirrer. The beaker was covered with aluminum foil and heated at 55°C for 3 hours while maintaining constant stirring at 1200 rpm. Afterward, the mixture was left to stand to allow separation of the upper and sedimentary phases. The upper phase was discarded, and the sedimentary phase was suspended in 70% methanol and neutralized with glacial acetic acid. Following neutralization, the mixture was filtered and washed five times with 70% ethanol via vacuum filtration, then washed again with absolute methanol and filtered. The resulting CMC was air-dried.

Loading of *Lacticasebacillus paracasei* into the formulated Nipa Hydrogel. A pure culture of *Lacticaseibacillus paracasei* was initially inoculated into a 250 mL Erlenmeyer flask containing MRS broth and incubated at 35–37°C for 48 hours until turbidity was observed. Following this, the formulation of the CMC Nipa Hydrogel was initiated according to the methodology established by Domingo et al. (2022). A solution containing 7% NaOH, 12% urea, and 81% distilled water was prepared in an Erlenmeyer flask and pre-cooled to -12.6°C. One gram of carboxymethylcellulose was then added to the solution and stirred at 1500 rpm for 10 minutes. The mixture was subsequently centrifuged at 8000 rpm for 20 minutes. After centrifugation, the solution was transferred to a beaker and neutralized with 10% sulfuric acid. The CMC solutions were sterilized via autoclaving, and all glassware was sterilized in a hot air oven at 160°C for 2 hours, followed by 30 minutes of UV treatment. The carbomer powder was also UV-treated before use.

To create a sterile environment and promote the exclusive growth of *L. paracasei*, 50 mL of the CMC solution was aseptically transferred to a beaker placed on a magnetic hotplate stirrer. Carbomer powder was gradually added to the CMC solution with continuous stirring until a smooth, homogeneous mixture was obtained. As gelation commenced, one drop of triethanolamine was introduced, followed by 50 mL of MRS broth pre-inoculated with *L. paracasei.* Once the desired viscosity was reached, the final solution was transferred into a sterile petri dish and stored at 4°C.

2.3. Collection, Animal Care, and Acclimatization of Experimental Animals

Before conducting the animal testing, approval was obtained from the Institutional Animal Care and Use Committee (IACUC) of the university. Once approved, 12 male ICR mice of uniform age and weight were sourced from Mariano Marcos State University – Laboratory Animal Care Facility (MMSU-LACF). Each treatment group consisted of three mice, serving as triplicates for the study. The mice were randomly assigned to different treatment groups to ensure unbiased results.

The ICR mice were housed individually in 12x12x10 plastic cages with wire mesh under controlled conditions of 22-25°C, 55-75% humidity, adequate ventilation, and a 12-hour light/dark cycle. Cages were cleaned biweekly with soap and water, following the standard operating procedure for disinfection and cage maintenance at MMSU-LACF. Each mouse received approximately 40 grams of pellets as food, and 15-20 mL of purified water was provided in drinking bottles.

Before the experiment commenced, all mice underwent an acclimatization period of five days under these controlled conditions. During this process, test animals were given free access to food pellets and water ad libitum.

 doi:10.20944/preprints202409.1941.v

2.4. Excision of Wounds in ICR Mice and Application of Treatments

The wound excision procedure followed the protocols established by Dai et al. (2011) and Rhea & Dunnwald (2020) in their Murine Excisional Wound Healing Model, with all surgical interventions performed under sterile conditions. Mice were restrained by gently grasping the base of their tail with the thumb and index finger and then placed on a secure surface such as a wire cage top or towel. The mouse's shoulders were held using the free hand, and the scruff of its neck was grasped near the skull to immobilize it. A light strain on the tail using the little finger ensured stability throughout the process.

Topical anesthesia was applied using lidocaine cream before each mouse was shaved in the dorso-lumbar region and sterilized with 70% alcohol. Circular full-thickness excision wounds, 2.5 cm wide and 0.2 cm deep, were created by grasping the marked skin with toothed forceps and dissecting it using a surgical blade and pointed scissors.

The day following the excisions, morphoanatomical changes in the wounds were recorded for assessment. Mice were then treated with the following: untreated but covered with gauze (Group I), Nipa hydrogel loaded with Nipa Indigenous Microorganisms (Group II), Nipa hydrogel with Lactobacillus plantarum (Group III), and a commercial hydrogel wound dressing, DuoDERM® (ConvaTec), with povidone-iodine (Group IV). Treatments were applied topically using a sterile cotton-tipped applicator, spreading evenly from the wound bed center outward to a thickness of 5mm. The wounds were then covered with a secondary gauze dressing, which remained in place for three to four days and was re-applied every few days over 21 days.

2.5. Assessment of the Wound Healing Activity

For the quantitative assessment, wound measurements of the mice were taken to assess the healing rate of the wounds. The area of the wound was measured using a vernier caliper, with a millimeter (mm) as the unit of measurement, these were done every two days. To calculate the reduction of the wound area in the study, Rabanal's (2007) formula was employed:

$$Healing\ Rate = \frac{Initial\ Wound\ Diameter\ (mm) - Final\ Wound\ Diameter\ (mm)}{Initial\ Wound\ Diameter\ (mm)} x100$$

2.6. Morphoanatomical Assessment of Wounded ICR Mice

The morphoanatomical assessment of the study encompassed two data sheets pertaining to the effectiveness of the different treatments by morphological assessment and histological examination. For the morphological assessment, the following qualitative criteria used in the studies by Andres (2004), Balicoco (2004), Cariaga (2008), Tabalbag (2012) and Simpliciano (2012) were adopted in determining the effectiveness of the treatments in healing wounds of mice: A (1) – Very red, very swollen and moist; B (2) – Red swollen and moist/presence of pus; C (3) – Red, slightly swollen and moist; D (4) – Swollen and moist/dry; E (5) – Scar formation and dry surface; F (6) – Presence of hair and wound healed completely.

2.7. Histological Assessment of Wounded ICR Mice

The histological examination, on the other hand, was performed and sent to the Mariano Marcos Memorial Hospital and Medical Center's (MMMMH & MC) Department of Pathology and Laboratories in Batac City, Ilocos Norte. A histological grading criterion adapted from Sultana et al., (2009) was also utilized (see Table 1).

 doi:10.20944/preprints202409.1941.v

Table 1. Histological grading criteria for healing according to Sultana et al.'s criteria.

Number	Histological Parameter
1	Amount of granulation tissue (profound-1, moderate-2, scanty-3, absent-4)
2	Inflammatory infiltrate (plenty-1, moderate-2, a few-3)
3	Collagen fiber orientation (vertical-1, mixed-2, horizontal-3)
4	Pattern of collagen (reticular-1, mixed-2, fascicle-3)
5	Amount of early collagen (profound-1, moderate-2, minimal-3)
6	Amount of mature collagen (profound-1, moderate-2, minimal-3)

Collection of Epidermal Tissue Sample. For the histological assessment, experimental animals were sacrificed via cervical dislocation, based on the guidelines for the use of cervical dislocation for rodent euthanasia by the University of Texas at Austin Institutional Animal Care and Use Committee (2020). First, a mouse was restrained in a normal standing position on a firm flat surface and the base of the tail was grasped firmly with one hand. Then, a sturdy stick-type pen, a rod-shaped piece of metal, or the thumb and first finger of the other hand were placed against the back of the neck at the base of the skull. In performing the dislocation, quickly push forward and down with the hand or object restraining the head while pulling backward with the hand holding the tail base. The effectiveness of 43 dislocations was verified by feeling for a separation of cervical tissues. When the spinal cord is severed, a 2-4 mm space will be palpable between the occipital condyles and the first cervical vertebra. After cervical dislocation, marked wound sites of the ICR mice were collected to evaluate the histological alterations using the criteria of Sultana. A longitudinal 4mm skin tissue sample was collected from the dorso-lumbar surface of each mouse. The remaining carcasses were then put inside labeled plastic bags and transferred to a suitable animal facility for appropriate disposal.

Preparation of Skin Tissue Samples for Histological Assessment. The preparation of skin tissue samples for histological assessment involved several key stages. Initially, tissue samples were preserved by fixation in 10% neutral buffered formalin overnight at room temperature to ensure structural integrity. Subsequently, the samples underwent a dehydration procedure to ensure complete removal of the fixative through immersion in 60-70% ethanol progressing through 90-95% ethanol for 15 minutes each and three changes of absolute ethanol for 15 minutes, 30 minutes, and 45 minutes. After which, xylene was utilized to remove the alcohol. The specimens were then subjected to wax infiltration and impregnated with molten paraffin wax in sequential stages of 20 minutes and 45 minutes. Once embedded in paraffin molds, the tissue blocks were cooled and sectioned using a rotary microtome. The resulting tissue sections were transferred to a warm water bath at 60-70°C and mounted onto slides for further histological analysis.

3. Results

3.1. Genomic Analysis

This study involved promoter analysis to support the utilization of *Lacticaseibacillus paracasei* BCRC-16100 into the hydrogel to determine the promoter elements responsible for the expression of genes linked with wound healing property of *L. paracasei* BCRC-16100.

Gene sodA and gsiC were identified to encode enzymes necessary during the process of wound healing. The sodA gene is typically a single-copy gene in most bacteria and is responsible for a significant portion of superoxide dismutase activity, while the gsiC gene encodes glutathione peroxidase. Wound healing occurs in three stages: inflammation, proliferation, and maturation. During the initial phase, neutrophils and macrophages are drawn to the injured tissue, producing reactive oxygen species (ROS) that have bactericidal effects on foreign substances in the wound. However, excessive ROS levels can damage tissue and hinder the healing process. Superoxide dismutase and glutathione peroxidase enzymes help neutralize superoxide anions, a type of ROS

 doi:10.20944/preprints202409.1941.v

derived from molecular oxygen. This reduces oxidative stress and creates an environment conducive to cell proliferation and migration, ultimately speeding up tissue repair (Jair et al., 2019; Iuchi et al., 2010; Camino-Sanz et al., 2021).

The two genes also had varying transcription frequencies, 7 (lexA, rpoD, cysB, carp, deoR, nagC and phoB) for sodA, while 4 (rpoD and phoB) for gsiC. The most dominant transcription factor among the two genes found was rpoD, which play a significant role in coordinating transcription of the two genes necessary for skin tissue repair (see Figure 1).

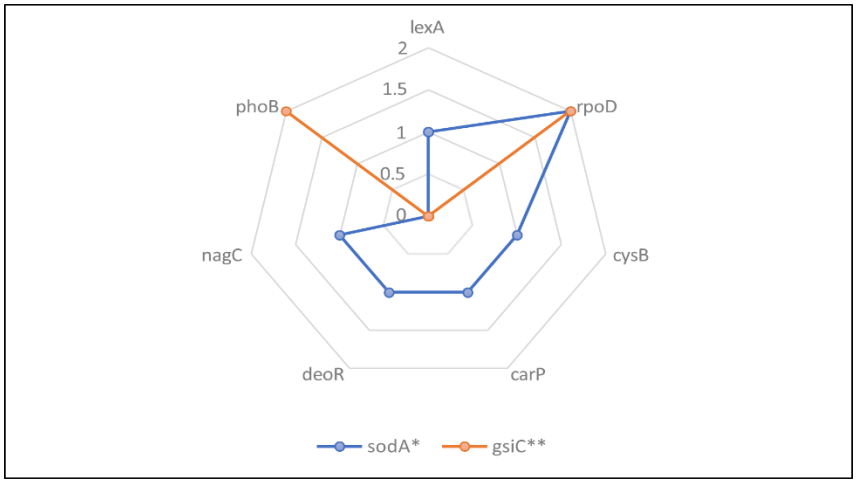

Figure 1. Transcription frequencies found in BCRC-16100 for skin tissue repair.

3.2. Morphoanatomical Assessment

To investigate its potential use for wound healing, NIMO-CH was evaluated in an in vivo wound healing model. All weights of the 12 ICR mice 51 were taken before wounding and treatment administration using a digital scale. After 21 days of observation period, their final weight was taken again to test if weight was a big factor to the wound healing process of the ICR mice. Statistical analysis found no significant differences in the mean weight of the experimental animals across treatment groups (see Table 2).

Table 2. Mean weight of ICR mice before and after the initiation of wound and treatment administration.

Treatment Groups	Initial Weight (g)	Final Weight (g)
Untreated (-)	32.30g	34.72
NIMO-CH	25.80g	28.52
DuoDERM (+)	29.02g	29.75
Significance	ns	ns
CV%	13.02	14.24

Legend: ns-not significant.

Excisional wounds inflicted on 12 ICR mice were divided into three groups – untreated, NIMO-CH treated, and DuoDERM Hydrogel treated with Povidone-Iodine for a period of 21 days. Measurements for their wound diameter were taken every 2 days, as well as the re-application of treatments. Morphological changes on the wound bed were observed following the criteria presented in the methodology chapter (see Tables 3 and 4).

At Day 2 observation period, all wounds among the different treatment groups exhibited very red, very swollen, and moist wound bed. Blood clots were also observed, following the first stage of wound healing, known as the exudative stage, to prevent bleeding and stop blood loss as stated by Wang et al., (2018). At Day 4, only treatments NIMO-CH and positive control group exhibited the presence of pus, whereas the negative group still exhibited very red and very swollen wound bed.

 doi:10.20944/preprints202409.1941.v

The presence of pus is a sign of the inflammatory stage of wound healing. This stage is where mast cells release granules filled with enzymes, histamine, and other active amines responsible for characteristic signs of inflammation, such as redness, heat, swelling, pain and clear fluid around the cut, which helps clean out the wound (Schultz et al., 2011).

Table 3. Mean morphological assessment on the wounds of ICR mice.

Treatment Groups	**Observation Period Day**									
	2	4	6	8	10	12	14	16	18	20
Untreated (-) Control	A	A	B	B	C	C	D	E	E	F
NIMO-CH	A	B	C	C	C	D	E	E	F	F
DuoDERM (+) control	A	B	C	C	C	D	D	E	E	F

Legend: A(1) – Very red, very swollen and moist. B (2) – Red, swollen and moist/presence of pus. C (3) – Red, slightly swollen and moist. D (4) – swollen and moist/dry. E (5) – Scar formation and dry surface. F (6) – Presence of hair and wound healed completely.

 doi:10.20944/preprints202409.1941.v

Table 4. Representative pictures of wound progression on ICR mice.

Treatment Groups	Observation Period Day									
	2	4	6	8	10	12	14	16	18	20
Untreated (-) Control	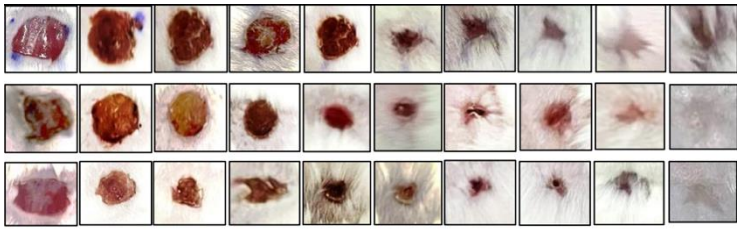									
NIMO-CH										
DuoDERM (+) Control										

On Day 6 to 12, redness and swollenness around the wound bed slightly decreased among the NIMO-CH and positive control groups, whereas the negative control group still exhibited red, swollen, and moist surface. Interestingly, wounds of the NIMO-CH started to dry first followed by the formation of scar at the fourteenth day. This is likely due to physiological activity of fibroblast cells actively producing collagen and glycosaminoglycans as stated by Wallace et al., (2023). These components form the foundation of wound bed, promoting stability and facilitating reepithelialization, which involves the migration of cells from wound periphery and adjacent edges. Initially, only a thin superficial layer of epithelial cells is laid down, but a thicker and more durable layer of cells will bridge the wound over time, resulting in scar formation.

On day 16, both the untreated group and the positive control group exhibited scar formation. On the eighteenth to twentieth day, the NIMO-CH group exhibited the presence of hair and complete wound healing. On the other hand, untreated and positive control groups only exhibited complete wound healing by the twentieth day of observation. Final pictures were taken, and only minimal scar pigmentation can be observed from NIMO-CH and positive control group.

Moreover, to further evaluate the effectivity of NIMO-CH in terms of quantitative data, healing rate of the different treatment groups was also assessed by measuring the wound contraction of the experimental animals every two days using a ruler in millimeters. All wounds began with a diameter of 2.5cm and a uniform depth. The percentage of wound healing was then calculated using the formula described in the methodology section (see Table 5).

On day 2, no wound closure was observed across all the treatment groups. On the fourth day, NIMO-CH group exhibited the highest mean percentage in wound closure with 12% healing rate, followed by the positive control group with 8% and 2% wound contraction rate for the untreated group. All treatment groups increased steadily over the period of 20 days.

Table 5. Mean percentage (%) healing within 20 days observation period.

Treatment Groups	Observation Period Day									
	2	4	6	8	10	12	14	16	18	20
Untreated (-) Control	0	2	15	21	60	68	75	80	87	90[b]
NIMO-CH	0	12	31	47	56	78	86	86	92	100[a]

 doi:10.20944/preprints202409.1941.v

DuoDERM (+) control	0	8	31	48	69	78	82	89	94	100[a]

Legend: * - significant at 5% level of significance. Ns – not significant.

Interestingly, on Day 10, the untreated group exhibited a higher percentage healing compared to the NIMO-CH group. This could be due to several factors, where the initial inflammatory response in the untreated wounds progressed more quickly, leading to a temporary increase in healing rate for the untreated group. NIMO-CH, on the other hand, might modulate the inflammatory response differently, potentially causing a slight delay in re-epithelialization (skin cell growth) around Day 10.

Overall, NIMO-CH and DuoDERM treatment groups were almost parallel in terms of their healing rate from Day 6 onwards. By day 20, all wounds in these two groups were completely healed. The untreated group, on the other hand, did not reach complete healing by the end of Day 20, only reaching a 90% wound contraction rate. Statistical analysis showed that the healing rate from the fourth day up to the eighteenth day are not significant, whereas the healing rate from the twentieth day are significant at 5% level of significance. Moreover, means from both the NIMO-CH and positive control group were not statistically significant from each other.

Furthermore, all treatments exhibited increased wound healing rates in ICR mice over time, as evidenced by the upward trend in their mean percentage healing. However, it's important to note that the untreated group did not achieve complete healing by day 20, unlike the NIMO-CH and DuoDERM groups (see Figure 2).

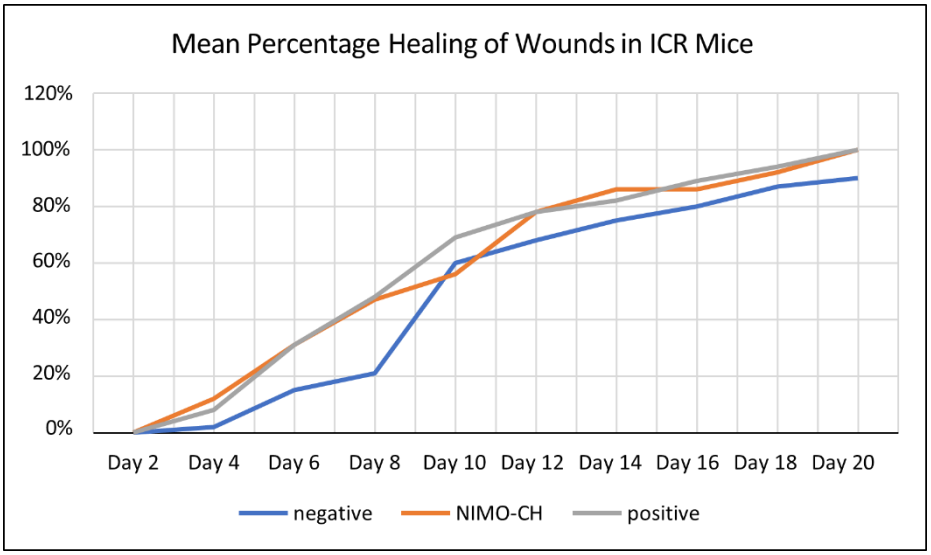

Figure 2. Trend on wound contraction rate among different treatment groups.

3.3. Histological Analysis

Monitoring wound progression over time is a critical aspect for studies focused on evaluating the efficacy of potential novel therapies, and histological examination of wounds is a very helpful tool to achieve this goal. Therefore, further analysis in terms of the histological features of the wounds in ICR mice were assessed after all observations were gathered. At the end of the 21-day period, all ICR mice were sacrificed via cervical dislocation and their skin tissue samples were collected and immediately fixed using 10% formalin in plastic sealed containers. All samples were given to MMMH and MC for slide preparation and interpretation.

The wound healing assessment data reveals promising progress across all three treatments. In terms of the amount of granulation tissue, all treatments show a consistent and profound amount, which suggests robust tissue regeneration. The graph also shows moderate levels of inflammatory infiltration across all three treatments (see Table 6 and Figure 3).

 doi:10.20944/preprints202409.1941.v

Table 6. Results of the histological analysis among the different treatment group.

Treatment Groups	Mean Score Histological Parameter				
	Amount of Granulation Tissue	Inflammatory Infiltrate	Collagen Fiber Orientation	Pattern of Collagen	Total Mean Score
Untreated (-) Control	4 Absent	3 Few	3 Horizontal	3 Fascicle	13
NIMO-CH	4 Absent	3 Few	2 Mixed	2 Mixed	11
DuoDERM (+) Control	4 Absent	3 Few	3 Mixed	3 Mixed	13
Significance	ns	ns	ns	ns	ns
CV %	10.65%	11.76%	22.59%	22.59%	11.58%

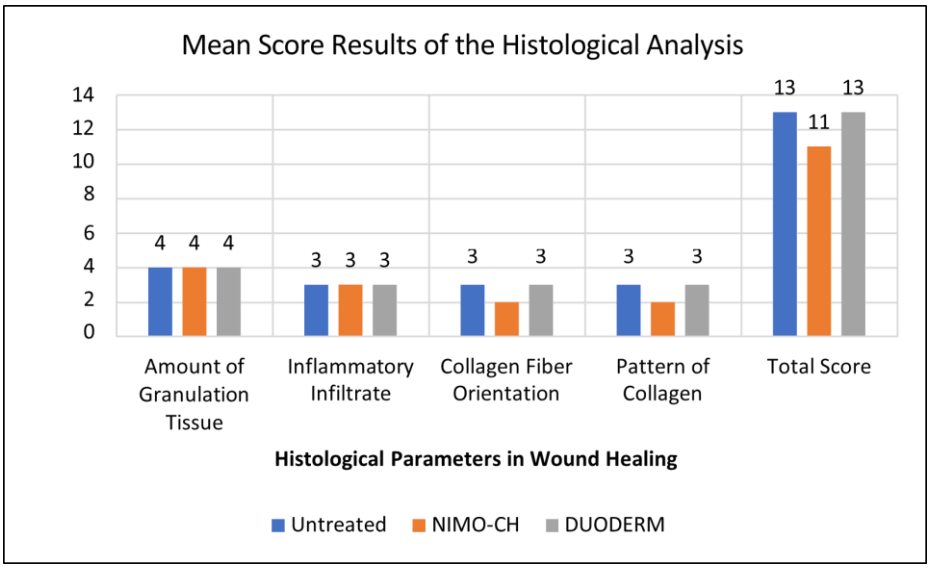

Figure 3. Graphical representation of the mean score results of the histological analysis.

4. Discussion

The findings of this study indicate that NIMO-CH loaded with *Lacticaseibacillus paracasei* demonstrates promising potential as an effective wound-healing treatment. Over a 21-day observation period, wound healing progression was meticulously monitored across three groups: untreated, NIMO-CH-treated, and DuoDERM Hydrogel-treated (positive control).

Statistical analysis indicates that the weight of the mice did not significantly impact the wound-healing process, thereby reinforcing the internal validity of the study and ruling out weight as a confounding variable. Throughout the wound healing stages, NIMO-CH exhibited effective progression, particularly in the exudative, inflammatory, and re-epithelialization stages. This is due to the present genes particularly gene soda and gsiC, in *L. paracasei* which are responsible for skin tissue repair. This finding is further supported by the observation that *L. paracasei* SGL 15 was found to significantly increase the growth of keratinocytes, which is the main cell type involved in re-epithelialization during wound healing (Brandi et al., 2020). The wound treated with NIMO-CH showed faster scar formation and complete healing by Day 20, comparable to DuoDERM-treated

 doi:10.20944/preprints202409.1941.v

wounds. Both treatments outperformed the untreated wounds, which lagged in wound closure and healing rate, achieving only 90% contraction by Day 20.

Histological analysis further supported these findings, as all treatments, including NIMO-CH, promoted the formation of granulation tissue—a critical component in tissue regeneration. Granulation tissue is essential for restoring the skin's dermal layer and orchestrating repair. As stated by Plikus et al., (2017) this complex tissue houses various cell types, extracellular matrix components, and growth factors that orchestrate repair and regeneration. Thus, this implies that all three treatments promoted healing by the formation of granulation tissue in the dermis.

Inflammatory infiltration was also observed at moderate levels in all treatments. The initial stage of wound healing triggers a cascade of immune responses. Neutrophils, macrophages, and lymphocytes, recruited from the bloodstream by injury signals infiltrate the wound site (Wang et al., 2022). These immune cells not only engulf invading pathogens but also secrete cytokines and growth factors, 59 promoting tissue repair and initiating the transition to the proliferation stage. Moderate inflammatory infiltrate observed in all groups reflects a balanced immune response, as expected during wound healing.

The collagen fiber orientation, which is crucial for the strength and functionality of the healed tissue, showed a mixed pattern across the treatments. According to Su et al., (2023), a well-organized collagen fiber with a basketweave pattern promotes stronger and more functional wound healing, whereas misaligned collagen fibers contribute to scar formation and reduced tissue function. While the presence of a mixed collagen fiber orientation observed in the analysis may suggest some potential for intermediate scarring, the presence of horizontal collagen fibers in certain areas indicated the possibility of stronger wound repair in other areas.

Statistically, no significant differences were found between the NIMO-CH and DuoDERM treatment groups, both in terms of wound contraction rates and histological parameters, suggesting that NIMO-CH is a viable alternative to conventional wound care treatments. Its comparable performance to the established positive control highlights its potential as an effective wound healing agent, particularly in reducing healing time, promoting scar formation, and modulating immune responses.

5. Conclusions

In conclusion, this study demonstrates the potential of NIMO-CH as a novel and promising wound-healing agent. It promoted wound healing in mice at a rate comparable to the commercially available product. Histological analysis further supported these findings, revealing similar wound-healing processes at the tissue level across all treatments. These combined results suggest that NIMO-CH may be a suitable and effective alternative for wound healing applications.

All authors have read and approved the final manuscript and consent to its publication.

Author Contributions: Abigail S. Castro: Conducted wound healing activity and writing of original draft. Alvin G. Domingo: Conceptualization, methodology and genome analysis. Jayson F. Cariaga: Cellulose extraction and hydrogel production. Francis A. Gamboa: Isolation and characterization of probiotics. Aira Cassandra S. Castro: Wound healing analysis. Aira Nadine Q. Pascua: Data curation and software analysis. Jimmbeth Zenila P. Fabia: Safety evaluation and identification of microorganism. Peter James Icalia Gann: Investigation, resources, and genome analysis. Bjorn S. Santos: Data Curation, funding acquisition. Shirley C. Agrupis: Supervision, and funding acquisition All authors have read and agreed to the published version of the manuscript.

Funding: This research was funded by the National Bioenergy Research and Innovation Center.

Data Availability Statement: The datasets generated and/or analyzed during the current study are available from the corresponding author on reasonable request.

Conflicts of Interest: The authors declare that they have no competing interests.

 doi:10.20944/preprints202409.1941.v

References

1. Asl, S., Mousavi, M., & Labbafi, M. (2017). Synthesis and Characterization of Carboxymethyl Cellulose from Sugarcane Bagasse. Journal of Food Processing & Technology, 08(08). https://doi.org/10.4172/2157-7110.1000687
2. Comino-Sanz, I. M., López-Franco, M. D., Castro, B., & Pancorbo-Hidalgo, P. L. (2021). The Role of Antioxidants on Wound Healing: A Review of the Current Evidence. *Journal of Clinical Medicine*, *10*(16). https://doi.org/10.3390/jcm10163558
3. Cariaga, J. F., Domingo, A. G., Santos, B. S., & Agrupis, S. C. (2023). Isolation of a - Cellulose from Nipa (Nypa fruticans Wurmb) Frond using Physico-Chemical Treatment. 16(23), 1754–1759. https://doi.org/10.17485/ijst/v16i23.2258
4. Dai, T., Kharkwal, G. B., Tanaka, M., Huang, Y.-Y., Bil, V. J., & Hamblin, M. R. (2011). Animal models of external traumatic wound infections. 2(4), 296–315. https://doi.org/10.4161/viru.2.4.16840
5. Domingo AG, Cariaga JF, Santos BS, Agrupis SC (2023) Production of Cellulose Hydrogel from Nipa (Nypa fruticans Wurmb) Frond. Indian Journal of Science and Technology 16(21): 1-8.
6. Iuchi, Y., Roy, D., Okada, F., Kibe, N., Tsunoda, S., Suzuki, S., … Fujii, J. (2010). Spontaneous skin damage and delayed wound healing in SOD1-deficient mice. Molecular and Cellular Biochemistry, 341(1-2), 181–194. doi:10.1007/s11010-010-0449-y
7. Jair, W., Lu, F., Huang, W., Pan, Y., Lin, L., Huang, H., & Yang, C. (2019). Roles of the Two-MnSOD System of Stenotrophomonas maltophilia in the Alleviation of Superoxide Stress. *International Journal of Molecular Sciences*, *20*(7). https://doi.org/10.3390/ijms20071770
8. Järbrink, K., Ni, G., Sönnergren, H., Schmidtchen, A., Pang, C., Bajpai, R., & Car, J. (2016). Prevalence and incidence of chronic wounds and related complications: a protocol for a systematic review. Systematic Reviews, 5(1). doi: 10.1186/s13643-016-0329-y
9. Jose, G., Shalumon, K. T., Chen, J.-P., & Yu, C. (2019). Natural Polymers Based Hydrogels for Cell Culture Applications. Current Medicinal Chemistry, 26. https://doi.org/10.2174/0929867326666190903113004
10. Martinengo L, Olsson M, Bajpai R, et al. (2019) Prevalence of chronic wounds in the general population: systematic review and meta-analysis of observational studies. Ann Epidemiol. 2019;29:8-15.
11. Plikus, M. V., Guerrero-Juarez, C. F., Ito, M., Li, Y. R., Dedhia, P. H., Zheng, Y., Shao, M., Gay, D. L., Ramos, R., Hsi, T.-C., Oh, J. W., Wang, X., Ramirez, A., Konopelski, S. E., Elzein, A., Wang, A., Supapannachart, R. J., Lee, H.-L., Lim, C. H., & Nace, A. (2017). Regeneration of fat cells from myofibroblasts during wound healing. Science, 355(6326), 748–752. https://doi.org/10.1126/science.aai8792
12. Rhea, L., & Dunnwald, M. (2020). Murine Excisional Wound Healing Model and Histological Morphometric Wound Analysis. (162). https://doi.org/10.3791/61616
13. Schultz, G. S., Chin, G. A., Moldawer, L., & Diegelmann, R. F. (2011). Principles of Wound Healing (R. Fitridge & M. Thompson, Eds.). PubMed; University of Adelaide Press. https://www.ncbi.nlm.nih.gov/books/NBK534261/
14. Su, C., Liu, T., Wang, H., & Yang, W. (2023). Histopathological Study on Collagen in Full-Thickness Wound Healing in Fraser's Dolphins (Lagenodelphis hosei). Animals, 13(10), 1681–1681. https://doi.org/10.3390/ani13101681
15. Sultana, J., Molla, M. R., Kamal, M., Shahidullah, M., Begum, F., & Bashar, M. A. (2009). Histological differences in wound healing in Maxillofacial region in patients with or without risk factors. Bangladesh Journal of Pathology, 24(1), 3–8. https://doi.org/10.3329/bjpath.v24i1.2874
16. Wallace, H., Basehore, B., & Zito, P. (2023). Wound Healing Phases. Statpearls Publishing. Retrieved from https://www.ncbi.nlm.nih.gov/books/NBK470443/
17. Wang, C., Wang, M., Xu, T., Zhang, X., Lin, C., Gao, W., Xu, H., Lei, B., & Mao, C. (2019). Engineering Bioactive Self-Healing Antibacterial Exosomes Hydrogel for Promoting Chronic Diabetic Wound Healing and Complete Skin Regeneration. Theranostics, 9(1), 65–76. https://doi.org/10.7150/thno.29766
18. Wang, Z., Qi, F., Luo, H., Xu, G., & Wang, D. (2022). Inflammatory Microenvironment of Skin Wounds. Frontiers in Immunology, 13. https://doi.org/10.3389/fimmu.2022.789274
19. Yaseen, H. S., Asif, M., Saadullah, M., Mahrukh, Asghar, S., Shams, M. U., Bazmi, R. R., Saleem, M., Yousaf, H. M., & Yaseen, M. (2020). Methanolic extract of Ephedra ciliata promotes wound healing and arrests inflammatory cascade in vivo through downregulation of TNF-α. Inflammopharmacology, 28(6), 1691–1704. https://doi.org/10.1007/s10787-020-00713-7